Spin-Wave Instabilities in Large-Scale Nonlinear Magnetization Dynamics

Giorgio Bertotti,[1] Isaak D. Mayergoyz,[2] and Claudio Serpico[3]

[1]Istituto Elettrotecnico Nazionale Galileo Ferraris, Corso M. d'Azeglio 42, I-10125 Torino, Italy

[2]Department of Electrical and Computer Engineering, University of Maryland, College Park, Maryland 20742

[3]INFM Unità di Napoli, and Department of Electrical Engineering, Università di Napoli "Federico II," I-80125 Napoli, Italy

(Received 4 April 2001; published 2 November 2001)

The stability of large magnetization motions in systems with uniaxial symmetry subject to a circularly polarized radio-frequency field is analytically studied. Instability conditions valid for arbitrary values of the amplitude and frequency of the driving field are derived. In the limit of small motions, these conditions yield Suhl's theory of spin-wave instabilities for the case of ferromagnetic resonance. It is shown that the input powers capable of inducing spin-wave instabilities are bounded from both below and above, so that large enough motions are always stable. In addition, it is demonstrated that stability of uniform motions depends on their preparation history.

DOI: 10.1103/PhysRevLett.87.217203 PACS numbers: 75.40.Gb, 05.45.–a, 76.50.+g

One of the central problems in ferromagnetism is the description of the various magnetization processes that set in when the external field is slowly reversed starting from saturation. In ideal single-crystal ellipsoids, free energy minimization shows that the magnetization is spatially uniform at saturation. Magnetization reversal is then studied by analyzing the stability of the uniform-magnetization state when the external field is slowly varied. Loss of stability may occur through uniform or nonuniform deviations from saturation [1].

To what extent a similar picture holds under rapidly varying fields is still an open problem. In particular, it is not clear under what conditions there may exist stable dynamic states analogous to static saturation, in the sense that large spatially uniform magnetization motions are realized. The main obstacle lies in the strongly nonlinear nature of the Landau-Lifshitz-Gilbert (LLG) equation governing the magnetization dynamics [2]. The problem is important in order to understand the nature of dynamic states in driven magnetic systems. At the same time, it has relevant technological implications. In fact, magnetic response in magnetic recording and magnetotransport applications crucially depends on the maximum range over which the magnetization can follow rapidly varying fields in a coherent fashion [3].

Spatially uniform dynamic states were originally discussed in relation to ferromagnetic resonance. Initially, it was assumed that a spatially uniform radio-frequency field would certainly induce a spatially uniform magnetic response. Later, it became clear that, because of the nonlinear nature of LLG dynamics, at sufficiently high input powers spatially uniform motions could get coupled to certain spin-wave modes, giving rise to complicated nonuniform magnetization configurations [4,5]. The main limitation of this analysis is that it was carried out for excited states close to static saturation. In this Letter, we present results for systems with uniaxial symmetry subject to fields of *arbitrary amplitude and frequency.* It would seem quite natural to suggest that if uniform motions are already unstable for weak excitations, they will be even more so under larger ones. However, this is not the case. Under large motions, the nature of the spin-wave perturbations is altered by the fact that they must remain orthogonal to the uniform motion at all times, in order to preserve the magnetization magnitude M_s. This physical mechanism affects the parametric resonance conditions governing instability and yields the remarkable consequence that the input powers capable of inducing spin-wave instabilities are bounded from *both below and above,* that is, large enough uniform motions are always stable.

The problem we study is that of a nonconducting ferromagnetic body subjected to a spatially uniform external field. The excitation conditions are such that displacement currents can be neglected. The body is of spheroidal shape, with uniaxial crystal anisotropy along the spheroid symmetry axis. The symmetry axis and the perpendicular plane will be denoted by the symbols "$\|$" and "$\perp$," respectively. The magnetization $\mathbf{M}$ obeys the LLG equation coupled to magnetostatic Maxwell equations. The LLG equation is written in the following dimensionless form:

$$\frac{\partial \mathbf{m}}{\partial t} - \alpha \mathbf{m} \times \frac{\partial \mathbf{m}}{\partial t} = -\mathbf{m} \times \mathbf{h}_{\text{eff}} , \qquad (1)$$

where $\mathbf{m} = \mathbf{M}/M_s$, $\mathbf{h}_{\text{eff}} = \mathbf{H}_{\text{eff}}/M_s$, time is measured in units of $(\gamma M_s)^{-1}$, M_s is the saturation magnetization, γ is the absolute value of the gyromagnetic ratio, α is the damping constant, and $\mathbf{m}$ has zero normal derivative at the body surface. The effective field is given by

$$\mathbf{h}_{\text{eff}} = \mathbf{h}_{a\perp}(t) + \mathbf{h}_M + (h_{a\|} + \kappa m_{\|})\mathbf{e}_{\|} + \nabla^2 \mathbf{m} , \qquad (2)$$

where κ is the anisotropy constant, $\mathbf{e}_{\|}$ is the unit vector along the symmetry axis, and spatial coordinates in the Laplacian $\nabla^2 \mathbf{m}$ are measured in units of the exchange length $l_{\text{EX}} = \sqrt{2A/\mu_0 M_s^2}$ (A is the exchange stiffness constant). The magnetostatic field $\mathbf{h}_M$ is obtained by solving Maxwell equations with appropriate boundary conditions.

Finally, the external field consists of the circularly polarized radio-frequency component $\mathbf{h}_{a\perp}(t)$, of amplitude $h_{a\perp}$ and angular frequency ω, and of the dc component $h_{a\parallel}\mathbf{e}_{\parallel}$.

It is quite remarkable that the problem described by Eqs. (1) and (2) *always* admits spatially uniform time-harmonic solutions for arbitrary values of $h_{a\parallel}$, $h_{a\perp}$, and ω [6]. These solutions, termed **P**-modes, represent dynamic states in which the magnetization $\mathbf{m}$ precesses around the symmetry axis $\mathbf{e}_{\parallel}$ in synchronism with the field. Therefore, a **P**-mode is simply identified by the deviation θ of $\mathbf{m}$ with respect to $\mathbf{e}_{\parallel}$ and by the lag angle ϕ of $\mathbf{m}_{\perp}$ with respect to $\mathbf{h}_{a\perp}$. These angles obey the equations [6]

$$\nu = \frac{h_{a\parallel} - \omega}{\cos\theta} + \kappa_{\mathrm{eff}}\,, \tag{3}$$

$$\nu^2 = \frac{h_{a\perp}^2}{\sin^2\theta} - \alpha^2\omega^2, \tag{4}$$

where $\nu = \alpha\omega\cot\phi$ and $\kappa_{\mathrm{eff}} = \kappa + N_{\perp} - N_{\parallel}$ ($N_{\perp}$ and $N_{\parallel}$ are the body demagnetizing factors). It is the existence of these explicit formulas for **P**-modes that enables one to study their stability in rigorous terms. Let us assume that a given **P**-mode of magnetization $\mathbf{m}_P$ is slightly distorted by the perturbation $\Delta\mathbf{m}$. The perturbation preserves the magnetization magnitude, which means that $\Delta\mathbf{m}\cdot\mathbf{m}_P = 0$. For this reason, we use the unit vectors $\mathbf{e}_1$ and $\mathbf{e}_2$ parallel to $d\mathbf{m}_P/dt \times \mathbf{m}_P$ and $d\mathbf{m}_P/dt$, respectively, as time-varying basis vectors: $\Delta\mathbf{m}(\mathbf{r},t) = a_1(\mathbf{r},t)\mathbf{e}_1(t) + a_2(\mathbf{r},t)\mathbf{e}_2(t)$. After substitution of $\mathbf{m}_P + \Delta\mathbf{m}$ into Eq. (1), linearization with respect to $\Delta\mathbf{m}$, and use of Eqs. (3) and (4) for $\mathbf{m}_P$, one obtains

$$\begin{pmatrix} 1 & \alpha \\ -\alpha & 1 \end{pmatrix}\frac{\partial}{\partial t}\begin{pmatrix} a_1 \\ a_2 \end{pmatrix} = \begin{pmatrix} 0 & 1 \\ -1 & 0 \end{pmatrix}\begin{pmatrix} \Delta h_{M1} \\ \Delta h_{M2} \end{pmatrix} + \begin{pmatrix} -\alpha\omega\cos\theta & -\nu + N_{\perp} + \nabla^2 \\ \nu - N_{\perp} - \nabla^2 - \kappa\sin^2\theta & -\alpha\omega\cos\theta \end{pmatrix}\begin{pmatrix} a_1 \\ a_2 \end{pmatrix}, \tag{5}$$

where $(\Delta h_{M1}, \Delta h_{M2})$ are the components of the perturbation magnetostatic field along $\mathbf{e}_1$ and $\mathbf{e}_2$, respectively.

The study of Eq. (5) for a generic perturbation is difficult. However, the most relevant perturbations are expected to be thermally generated spin waves of the form $\Delta\mathbf{m}(\mathbf{r},t) = \mathbf{c}_q(t)\cos[\mathbf{q}\cdot(\mathbf{r} - \mathbf{r}_q)]$. The main limitation is that plane-wave perturbations are generally not compatible with the boundary conditions of the problem. However, boundary conditions will produce additional magnetostatic fields that are concentrated in a thin boundary layer with thickness $\sim\lambda$, which yields negligible effects if $\lambda \ll L$, where L measures the typical linear dimensions of the body [4]. Therefore, our analysis will hold for $|\mathbf{q}| \geq q_{\min}$, where $q_{\min} \sim 2\pi l_{\mathrm{EX}}/L$. In addition, we will study uniform perturbations $\Delta\mathbf{m}(\mathbf{r},t) = \mathbf{c}_0(t)$, for which boundary conditions can be exactly taken into account with no difficulty. Spin waves of wavelength close to the atomic scale cannot be treated by the continuous semiclassical approach underlying Eq. (1). Their presence is indirectly taken into account through the values assumed for the saturation magnetization M_s and the damping constant α [7].

By substituting $a_{1,2}(\mathbf{r},t) = c_{q1,q2}(t)\cos[\mathbf{q}\cdot(\mathbf{r} - \mathbf{r}_q)]$ into Eq. (5) and by calculating the magnetostatic field $\Delta\mathbf{h}_M$ due to $\nabla\cdot\Delta\mathbf{m}$ inside the body, one finds

$$\frac{d}{dt}\begin{pmatrix} c_{q1} \\ c_{q2} \end{pmatrix} = A_q\begin{pmatrix} c_{q1} \\ c_{q2} \end{pmatrix} + \frac{1}{1+\alpha^2}\begin{pmatrix} 1 & -\alpha \\ \alpha & 1 \end{pmatrix} \times [R_1(t) + R_2(t)]\begin{pmatrix} c_{q1} \\ c_{q2} \end{pmatrix}, \tag{6}$$

$$A_q = \frac{1}{1+\alpha^2}\begin{pmatrix} 1 & -\alpha \\ \alpha & 1 \end{pmatrix} \times \begin{pmatrix} -\alpha\omega\cos\theta & -\nu_q \\ \nu_q - \kappa_q\sin^2\theta & -\alpha\omega\cos\theta \end{pmatrix}, \tag{7}$$

$$R_1 = -\frac{\sin 2\theta_q}{2}\begin{pmatrix} \sin\theta\sin\omega t & 0 \\ \sin 2\theta\cos\omega t & -\sin\theta\sin\omega t \end{pmatrix}, \tag{8}$$

$$R_2 = \frac{\sin^2\theta_q}{2}\begin{pmatrix} \cos\theta\sin 2\omega t & \cos 2\omega t \\ \cos^2\theta\cos 2\omega t & -\cos\theta\sin 2\omega t \end{pmatrix}, \tag{9}$$

where θ_q is the angle between $\mathbf{q}$ and $\mathbf{e}_{\parallel}$ and

$$\nu_q = \nu - N_{\perp} + q^2 + \frac{\sin^2\theta_q}{2}\,, \tag{10}$$

$$\kappa_q = \kappa - 1 + \frac{3\sin^2\theta_q}{2}\,. \tag{11}$$

Uniform perturbations obey the much simpler equation $dc_0/dt = A_0 c_0$, $c_0(t) \equiv [c_{01}(t), c_{02}(t)]$, where A_0 is formally identical to Eq. (7), with ν and κ_{eff} in place of ν_q and κ_q, respectively.

The key information about spin-wave instabilities is carried by the one-period map [8] associated with Eq. (6). Given the fundamental matrix solution $C_q(t)$ of Eq. (6), with $C_q(0) = \delta_{ij}$, the one-period map M_q is defined as $M_q = C_q(2\pi/\omega)$. Stability is controlled by the eigenvalues of M_q, the characteristic multipliers $\mu_{\pm}$. The system becomes unstable whenever $|\mu_+| \geq 1$ or $|\mu_-| \geq 1$. Therefore, one can immediately determine the stability of *all* **P**-modes with respect to any particular spin-wave perturbation by numerical integration of Eq. (6) (see Fig. 1). According to the general properties of one-period maps, $\det M_q \equiv \mu_+\mu_- = \exp(2\pi\,\mathrm{tr}A_q/\omega)$, provided R_1 and R_2 have zero average over one period. Therefore, the system is always unstable for $\mathrm{tr}A_q > 0$. On the contrary, for $\mathrm{tr}A_q \leq 0$ one observes a remarkably rich pattern typical of parametric resonance [9], with instability concentrated along *Arnold tongues.* The origin of this result can be comprehended by analyzing the structure of Eq. (6) in the region $\mathrm{tr}A_q \leq 0$.

Let us first study Eq. (6) when one neglects R_1 and R_2. In that case the equation has constant coefficients and can

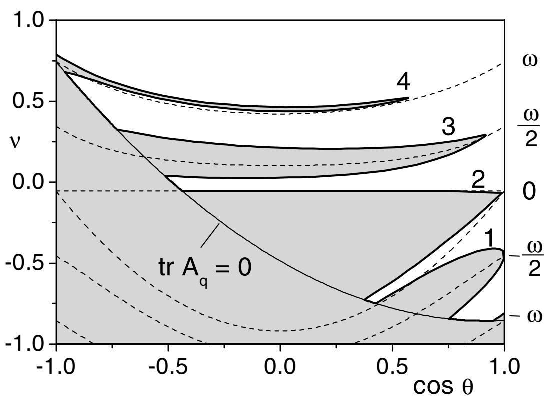

FIG. 1. Gray region: **P**-modes unstable with respect to spin-wave perturbations with $q^2 = 0.01$ and $\sin\theta_q = 0.3$, determined by numerical integration of Eq. (6). Parameters: $N_\perp = 0$, $\kappa = 0$, $\alpha = 0.01$, $\omega = 0.8$. Dashed lines: $\omega_q = 0$, $\omega_q = \pm\omega/2$, $\omega_q = \pm\omega$, where ω_q is given by Eq. (13). Numbers 1 through 4: parametric resonance order n.

be completely solved by standard methods. The associated one-period multipliers, $\mu_\pm^{(0)}$, are given by

$$\mu_\pm^{(0)} = \exp\left(\frac{\pi\,\mathrm{tr}A_q}{\omega}\right)\left(\cos\frac{2\pi\omega_q}{\omega} \pm i\sin\frac{2\pi\omega_q}{\omega}\right), \quad (12)$$

$$\omega_q^2 = \frac{1}{(1+\alpha^2)^2}\left[\left(\nu_q - \kappa_q\frac{\sin^2\theta}{2} - \alpha^2\omega\cos\theta\right)^2 - (1+\alpha^2)\kappa_q^2\frac{\sin^4\theta}{4}\right], \quad (13)$$

where $\omega_q^2 \equiv \det A_q - (\mathrm{tr}A_q)^2/4$ by definition. Equations formally identical to Eqs. (12) and (13), with ω_0, A_0, ν, and κ_{eff} in place of ω_q, A_q, ν_q, and κ_q, respectively, also describe stability with respect to uniform perturbations. Equation (13) represents the spin-wave dispersion relation in the time-dependent basis $(\mathbf{e}_1, \mathbf{e}_2)$. This relation explicitly depends on $\cos\theta$ and $\cot\phi$, i.e., on the particular **P**-mode considered, as a consequence of the fact that we deal with elementary excitations above far-from-equilibrium driven modes. According to Eq. (12), the system becomes unstable for $\omega_q^2 \le -(\mathrm{tr}A_q)^2/4$.

When R_1 and R_2 are included in the analysis, the equation for $C_q(t)$ becomes an equation with time-varying coefficients for which no general solution is known. Nevertheless, an approximate result can be obtained by a series expansion of which we were able to calculate the zeroth-order and first-order terms in closed form. As a result, we found for the characteristic multipliers:

$$\mu_\pm^{(1)} = \exp\left(\frac{\pi\,\mathrm{tr}A_q}{\omega}\right) \times \left(\cos\frac{2\pi\omega_q}{\omega} \pm \sqrt{Z_q^2 - 1}\,\sin\frac{2\pi\omega_q}{\omega}\right), \quad (14)$$

where $Z_q = K_1/(\omega^2/4 - \omega_q^2) + K_2/(\omega^2 - \omega_q^2)$, K_1 and K_2 representing certain regular functions of $\cos\theta$ and ν. The similarity with Eq. (12) is striking. According to Eq. (14), the system becomes unstable for negative ω_q^2, in a region which represents the first-order correction to $\omega_q^2 \le -(\mathrm{tr}A_q)^2/4$. In addition, parametric instability becomes possible around $\omega_q = \pm\omega/2$ and $\omega_q = \pm\omega$, where $Z_q \to \infty$ (dashed lines in Fig. 1). Indeed, we verified that Eq. (14) reproduces remarkably well the detailed structure of Arnold tongues determined numerically (Fig. 1).

The first-order calculation predicts five instability regions associated with $\omega_q = -\omega$, $-\omega/2$, 0 (i.e., negative ω_q^2), $\omega/2$, ω. Figure 1 shows that the $-\omega$ instability plays an irrelevant role. The other four would be described by the typical parametric resonance sequence [9] $n\omega/2$, $n = 1, 2, 3, 4$, in a time-independent vector basis, because the basis $(\mathbf{e}_1, \mathbf{e}_2)$ is rotated at the angular frequency ω. In principle, also instabilities with $n = 5, 6, \ldots$ are possible. However, they are expected to be much weaker, because they come from higher-order terms of the series expansion. In addition, their appearance may be ruled out by the limited range of variation of $\cos\theta$. We verified numerically that they are absent for $\omega = 0.8$ and $\alpha = 0.01$ and start to play some limited role for $\omega \sim 1$ and $\alpha \lesssim 0.001$.

The complete **P**-mode stability diagram is obtained by combining the diagram for uniform perturbations [i.e., $\mathrm{tr}A_0 \ge 0$, $\omega_0^2 \le -(\mathrm{tr}A_0)^2/4$] with all the diagrams for spin waves with $0 \le \sin^2\theta_q \le 1$ and $q^2 \ge q_{\mathrm{min}}^2$. Remarkably, the only place where q^2 appears in the entire analysis is Eq. (10). Therefore, given the stability diagram for a particular value of $\sin\theta_q$ and $q^2 = q_{\mathrm{min}}^2$, all the diagrams for larger values of q^2 are immediately obtained by a simple downward shift in the $(\cos\theta, \nu)$ plane. Figure 2 shows the result of this analysis for a thin film disk with negligible crystal anisotropy. **P**-modes in region **U** are made unstable by uniform perturbations, those in regions $\mathbf{S}_{12}$ and $\mathbf{S}_{34}$ by spin-wave parametric resonance of order $n = 1, 2$ and $n = 3, 4$, respectively. Figure 3 was

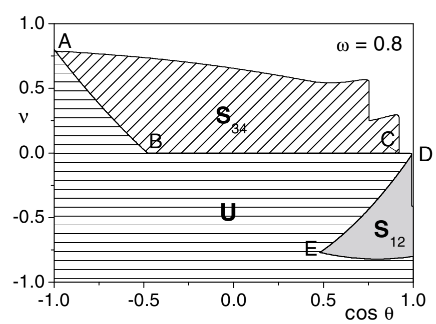

FIG. 2. **P**-mode stability diagram for a soft thin film disk. Parameters: $N_\perp = 0$, $\kappa = 0$, $\alpha = 0.01$, $\omega = 0.8$, $q_{\mathrm{min}}^2 = 0.01$. **U**: **P**-modes unstable with respect to uniform perturbations. $\mathbf{S}_{12}$ and $\mathbf{S}_{34}$: **P**-modes unstable because of spin-wave parametric resonance of order $n = 1, 2$ and $n = 3, 4$, respectively. Points A through E are indicated for the sake of comparison with Fig. 3. Detailed structure of $\mathbf{S}_{12}$ for $\cos\theta \simeq 1$, not visible in the figure, results in regions **I** and **II** of Fig. 3.

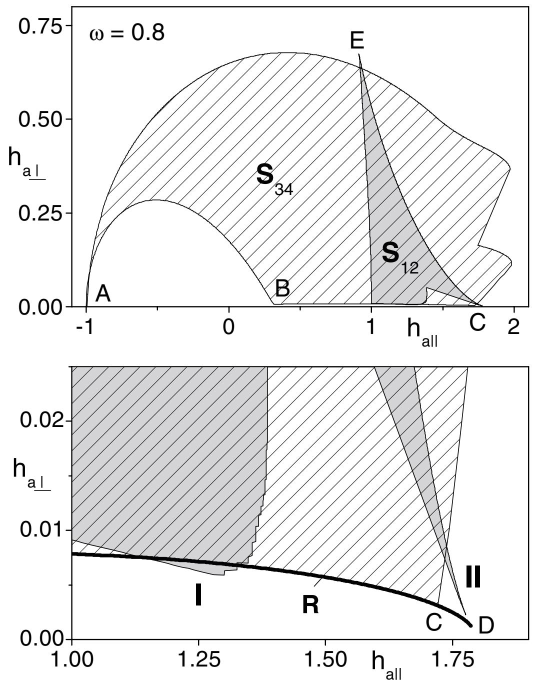

FIG. 3. Regions $\mathbf{S}_{12}$ and $\mathbf{S}_{34}$ of Fig. 2, as they appear in the $(h_{a\parallel}, h_{a\perp})$ plane. Bottom: Magnified view of ferromagnetic resonance region. **R**: Riemann cut. CD: foldover segment. **I** and **II**: first-order and second-order Suhl's instabilities.

obtained by using Eqs. (3) and (4) to transform Fig. 2 from the **P**-mode plane $(\cos\theta, \nu)$ to the control plane $(h_{a\parallel}, h_{a\perp})$ of interest in experiments. Remarkably enough, regions $\mathbf{S}_{12}$ and $\mathbf{S}_{34}$ fill out only a limited part of the control plane. This occurs because the system is stable for large positive ν (see Fig. 2), as a result of the absence of high-order parametric instabilities. In thin films $(N_\perp = 0)$, the approximate location of the upper instability boundary of Fig. 2 can be estimated through Eqs. (10) and (13) by neglecting terms proportional to α^2 and by assuming that $\kappa_q < 0$ for the spin-wave modes responsible for the $\omega_q = \omega$ instability: $\nu \le \nu_q \le \omega_q = \omega$. By inserting this result into Eqs. (3) and (4), one concludes that the system can be unstable only if $h_{a\perp}^2 \le \omega^2 \sin^2\theta$ and $(h_{a\parallel} - \omega)/\cos\theta + \kappa_{\text{eff}} \le \omega$. Whenever the excitation conditions are outside this range, the system will certainly be stable.

The transformation from Fig. 2 to Fig. 3 is not one to one, because there are two or four **P**-modes associated with each pair $(h_{a\parallel}, h_{a\perp})$ [see Eqs. (3) and (4)]. Therefore, **P**-mode properties in the $(h_{a\parallel}, h_{a\perp})$ plane are defined on a Riemann surface with two or four folded sheets. If one considers a **P**-mode which is stable in the limit $h_{a\parallel} \to +\infty$ and then slowly decreases $h_{a\parallel}$, one will encounter $\mathbf{S}_{34}$ but not $\mathbf{S}_{12}$ if one remains above the line **R** of Fig. 3. This line acts as a Riemann cut in the control plane. Region $\mathbf{S}_{12}$ lies on a different sheet of the Riemann surface and can be reached only by approaching the line **R** from below. This is the region where first-order (**I**) and second-order (**II**) Suhl's instabilities [4] occur. Finally, the system undergoes uniform loss of stability when it crosses the segment CD. This segment identifies the conditions for which foldover [10] is observed in ferromagnetic resonance experiments.

The authors thank Pavel Kabos for inspiring suggestions. This research was supported in part by the U.S. Department of Energy, Engineering Research Program, and by the U.S. Department of Defense.

[1] A. Aharoni, *Introduction to the Theory of Ferromagnetism* (Oxford University Press, Oxford, 1996), Chap. 9; G. Bertotti, *Hysteresis in Magnetism* (Academic Press, San Diego, 1998), Chap. 11.
[2] See, for example, A. G. Gurevich and G. A. Melkov, *Magnetization Oscillations and Waves* (CRC Press, Boca Raton, FL, 1996), Chap. 2.
[3] For up-to-date reviews, see J. C. Mallinson, *Magneto-Resistive Heads* (Academic Press, San Diego, 1995); S. X. Wang and A. M. Taratorin, *Magnetic Information Storage Technology* (Academic Press, San Diego, 1999), and references therein.
[4] H. Suhl, Proc. IRE **44**, 1270 (1956); H. Suhl, J. Phys. Chem. Solids **1**, 209 (1957).
[5] *Nonlinear Phenomena and Chaos in Magnetic Materials,* edited by P. E. Wigen (World Scientific, Singapore, 1994), and references therein; H. Suhl and X. Y. Zhang, Phys. Rev. Lett. **57**, 1480 (1986); R. D. McMichael and P. E. Wigen, Phys. Rev. Lett. **64**, 64 (1990).
[6] G. Bertotti, C. Serpico, and I. D. Mayergoyz, Phys. Rev. Lett. **86**, 724 (2001).
[7] H. B. Callen, J. Phys. Chem. Solids **4**, 256 (1958); H. Suhl, IEEE Trans. Magn. **34**, 1834 (1998).
[8] J. Hale and H. Kocak, *Dynamics and Bifurcations* (Springer-Verlag, Berlin, 1991), Sec. 8.6.
[9] V. I. Arnold, *Mathematical Methods of Classical Mechanics* (Springer-Verlag, Berlin, 1989), p. 113.
[10] D. J. Seagle, S. H. Charap, and J. O. Artman, J. Appl. Phys. **57**, 3706 (1985); Y. K. Fetisov, C. E. Patton, and V. T. Sygonach, IEEE Trans. Magn. **35**, 4511 (1999).